JBC Papers in Press. Published on April 16, 2015 as Manuscript M115.655043
The latest version is at http://www.jbc.org/cgi/doi/10.1074/jbc.M115.655043

A POINT MUTATION IN THE UBIQUITIN LIGASE RNF170 THAT CAUSES AUTOSOMAL DOMINANT SENSORY ATAXIA DESTABILIZES THE PROTEIN AND IMPAIRS INOSITOL 1,4,5-TRISPHOSPHATE RECEPTOR-MEDIATED Ca^{2+} SIGNALING

Forrest A. Wright, Justine P. Lu, Danielle A. Sliter,[2] Nicolas Dupré,[3] Guy A. Rouleau[4] and Richard J.H. Wojcikiewicz[1]

From Department of Pharmacology, SUNY Upstate Medical University, Syracuse, NY 13210, USA

Running title: Effects of an RNF170 mutation that causes neurodegeneration

[1]To whom correspondence should be addressed: Department of Pharmacology, SUNY Upstate Medical University, 750 E. Adams St., Syracuse, NY 13210, USA. Phone: 315-464-7956; Fax: 315-464-8014; E-mail: wojcikir@upstate.edu
[2] NINDS, NIH, Bethesda, MD 20892, USA
[3] Neuromuscular and Neurogenetic Disease Clinic, CHU de Québec, Laval University, Quebec City, QC, Canada
[4] Montreal Neurological Institute and Hospital and Department of Neurology and Neurosurgery, McGill University, Montreal, QC, Canada

Keywords: ubiquitin ligase, ER, mutant, neurodegenerative disease, protein stability, calcium intracellular release, InsP3R

Background: RNF170 is an endoplasmic reticulum membrane ubiquitin ligase that when mutated at arginine199 causes a neurodegenerative disease.
Results: The mutation disrupts salt bridges between transmembrane domains, destabilizes the protein and inhibits Ca^{2+} signaling via IP_3 receptors.
Conclusion: These manifestations of the mutation are likely causative to neurodegeneration.
Significance: Understanding the mechanism of action of mutant ubiquitin ligases will lead to better therapies.

RNF170 is an endoplasmic reticulum membrane ubiquitin ligase that contributes to the ubiquitination of activated inositol 1,4,5-trisphosphate (IP_3) receptors, and that also, when point mutated (arginine to cysteine at position 199), causes autosomal dominant sensory ataxia (ADSA), a disease characterized by neurodegeneration in the posterior columns of the spinal cord. Here we demonstrate that this point mutation inhibits RNF170 expression and signaling via IP_3 receptors. Inhibited expression of mutant RNF170 was seen in cells expressing exogenous RNF170 constructs and in ADSA lymphoblasts, and appears to result from enhanced RNF170 autoubiquitination and proteasomal degradation. The basis for these effects was probed via additional point mutations, revealing that ionic interactions between charged residues in the transmembrane domains of RNF170 are required for protein stability. In ADSA lymphoblasts, platelet-activating factor-induced Ca^{2+} mobilization was significantly impaired, while neither Ca^{2+} store content, IP_3 receptor levels, nor IP_3 production were altered, indicative of a functional defect at the IP_3 receptor locus, which may be the cause of neurodegeneration. CRISPR/Cas9-mediated genetic deletion of RNF170 showed that RNF170 mediates the addition of all of the ubiquitin conjugates known to become attached to activated IP_3 receptors (monoubiquitin and Lys-48- and Lys-63-linked ubiquitin chains), and that wild-type and mutant RNF170 have apparently identical ubiquitin ligase activities towards IP_3 receptors. Thus, the Ca^{2+} mobilization defect seen in ADSA lymphoblasts is apparently not due to aberrant IP_3 receptor ubiquitination. Rather, the defect likely reflects abnormal ubiquitination of other substrates, or adaptation to the chronic reduction in RNF170 levels.

Copyright 2015 by The American Society for Biochemistry and Molecular Biology, Inc.

Downloaded from http://www.jbc.org/ at Shanghai Information Center for Life Sciences, Chinese Academy of Sciences on May 25, 2015

In eukaryotic cells, ubiquitin ligases (E3s) work together with ubiquitin-conjugating enzymes (E2s) to promote ubiquitination of a range of substrates, often leading to their degradation by the proteasome [1-5]. Mammals express hundreds of E3s, the vast majority of which contain a RING domain, a motif that appears to provide a docking site for E2s and be necessary for ubiquitin transfer to the substrate [3-5]. Endoplasmic reticulum (ER)-associated degradation (ERAD) is the term used to describe the pathway by which aberrant ER lumen or membrane proteins are removed from the cell via ubiquitination and proteasomal degradation [6,7]. A recent bioinformatic survey of RING domain-containing proteins that localize to the ER membrane and which could play a role in ERAD identified a group of 24 E3s [8], some of which (e.g. HRD1) appear be capable of mediating the ubiquitination of a broad array of substrates, while others (e.g. TRC8) have a much narrower substrate range [3,6,7]. Further, several of the E3s identified (e.g. RNF170) have yet to be fully characterized [8].

Inositol 1,4,5-trisphosphate receptors (IP_3Rs) are ER membrane proteins that form tetrameric Ca^{2+} channels that govern ER Ca^{2+} store release [9,10]. When persistently activated, a portion of cellular IP_3Rs are ubiquitinated and degraded by the proteasome apparently via the ERAD pathway, and this IP_3R "down-regulation" suppresses Ca^{2+} mobilization [11,12]. Recent studies on the mechanism of IP_3R processing by the ERAD pathway have shown that a complex composed of the integral ER membrane proteins erlin1 and erlin2 associates rapidly with activated IP_3Rs [11-14], as does RNF170 [15]. RNF170 is ~ 257 amino acids in length, is highly conserved in mammals, is predicted to have 3 transmembrane (TM) domains, with the RING domain facing the cytosol [15,16], and is constitutively associated with the erlin1/2 complex. RNF170 contributes to IP_3R ubiquitination [15], although whether it is responsible for the addition of all of the conjugates that become attached to activated IP_3Rs (monoubiquitin and Lys-48- and Lys-63-linked ubiquitin chains) [17,18] is currently unknown. Remarkably, a recent molecular genetic study demonstrated that autosomal dominant sensory ataxia (ADSA), a rare neurodegenerative disease characterized by ataxic gait, reduced sensory perception, and neurodegeneration in the posterior columns of the spinal cord, segregates with an arginine (R^{199}) to cysteine mutation in human RNF170 [16,19]. Here we examine the effects of this mutation on the properties of RNF170 and find that it destabilizes the protein because of disruption of a salt bridge between TM domains 2 and 3, and that mutant RNF170 disrupts Ca^{2+} signaling at the IP_3R locus in ADSA lymphoblasts. Genetic deletion of RNF170 revealed that RNF170 mediates the addition of all ubiquitin conjugates to activated IP_3Rs and that the ubiquitin ligase activities of wild-type and mutant RNF170 towards activated IP_3Rs are apparently identical. Thus, aberrant ubiquitination of other substrates, or cellular adaptation to chronically reduced RNF170 levels likely accounts for the ADSA-associated Ca^{2+} signaling deficit.

Experimental procedures

Materials – Hela cells were cultured as described [13]. Human lymphoblast cell lines were isolated from control and affected individuals [16] and were cultured in Iscove's Modified Dulbecco's Medium (Thermo Scientific) supplemented with 10% fetal bovine serum, 50 units/ml penicillin, 50 μg/ml streptomycin, and 1mM L-glutamine. Lymphoblasts were cultured in flasks, were fed every 2-3 days and were subcultured 1:10 once per week. Lipofectamine was from Invitrogen, anti-FLAG epitope clone M2 was from Sigma, anti-HA epitope clone HA11 was from Covance, anti-ubiquitin clone FK2 and MG-132 were from BioMol International, anti-RNF170, anti-erlin1, anti-erlin2, anti-Hrd1, anti-gp78, anti-IP_3R1 and anti-IP_3R2 were prepared as described [13-15,20], anti-β-tubulin was from Cell Signaling Technology, anti-p97 was from Research Diagnostics Inc., anti-p53 clone DO-1 was from Santa Cruz Biotech., anti-IP_3R3 was from BD Biosciences, anti-Lys-48 and anti-Lys-63 linkage-specific antibodies were a generous gift from Genentech, anti-IP_3R1-3, which recognizes all IP_3R types equally well [21], was a generous gift from Dr Jan Parys (KU Leuven, Belgium), endoglycosidase H (endo H) was from New England Biolabs, and fura2-AM, cycloheximide (CHX), platelet-activating factor (PAF) and gonadotropin-releasing hormone (GnRH) were from Sigma.

Downloaded from http://www.jbc.org/ at Shanghai Information Center for Life Sciences, Chinese Academy of Sciences on May 25, 2015

Plasmids – Mouse and human RNF170 cDNAs were cloned from mouse αT3 cells and human lymphoblasts as described [15]. $RNF170^{FLAG}$ was constructed by ligating the sequence encoding 257 amino acid mouse RNF170 into the *Kpn*1 and *Bam*H1 sites of the pCMV14-3xFLAG expression vector such that a triple FLAG tag (DYKDHDGDYKDHDIDYKDDDDKG) is spliced to the C-terminus [15]. $RNF170^{HA}$ was constructed by PCR amplification of mouse and human RNF170 cDNAs, such that an HA tag (GYPYDVPDYAG) is spliced to the C-terminus. Additional constructs were created via PCR that encode proteins with an optimal *N*-glycosylation consensus sequence (NSTMMS) [22] immediately after the HA tag, and with a variety of amino acid substitutions. Primer sequences are available upon request.

Expression and analysis of RNF170 constructs – To analyze the expression of exogenous RNF170 and its mutants, HeLa cells (750,000 per well of a 6-well plate) were transfected (7µl Lipofectamine plus 4.8µg total DNA), and 24-48h later cells were collected with 155 mM NaCl, 10mM HEPES, 1mM EDTA, pH 7.4. Cells were then centrifuged (2,300 x g for 1 min), were disrupted for 30 min at 4ºC with lysis buffer (150 mM NaCl, 50 mM Tris-HCl, 1 mM EDTA, 1% Triton-X100, 10 µM pepstatin, 0.2 mM PMSF, 0.2 µM soybean trypsin inhibitor, 1mM dithiothreitol, pH 8.0), were centrifuged (16,000 x g for 10 min at 4ºC), and supernatant samples were subjected to SDS-PAGE and immunoblotting as described [13-15]. For studying the interaction between the erlin1/2 complex and RNF170 by co-immunoprecipitation [15], cells were disrupted using lysis buffer that contained 1% CHAPS instead of Triton-X100. The ubiquitin ligase activity of immunopurified $RNF170^{FLAG}$ constructs was assessed as described [15].

Lymphoblasts – To assess protein expression in cell lysates, lymphoblasts were collected by centrifugation (1,000 x g for 5 min), were washed once by resuspension in PBS followed by centrifugation (16,000 x g for 1 min), were disrupted for 30 min at 4ºC with 1% CHAPS lysis buffer, were centrifuged (16,000 x g for 10 min at 4ºC), and supernatant samples were subjected to SDS-PAGE and immunoblotting as described [13-15]. For measurement of cytosolic free Ca^{2+} concentration ($[Ca^{2+}]_c$), lymphoblasts were collected by centrifugation (1,000 x g for 1 min), were washed once and then incubated in culture medium at 2mg protein / ml with 5µM fura2-AM for 1h at 37ºC, were washed 4 times with Krebs HEPES buffer [23], and finally were resuspended at 0.5mg protein / ml in Krebs HEPES buffer for measurement of $[Ca^{2+}]_c$ at 37ºC, as described [23]. For measurement of IP_3 levels, lymphoblasts were collected by centrifugation (1,000 x g for 5 min), were washed once by resuspension in RPMI-1640 (Cellgro) followed by centrifugation (1,000 x g for 5 min), were resuspended in RPMI-1640 and pre-incubated at 37ºC for 1h, were then exposed to vehicle (DMSO) or PAF, and IP_3 mass was measured as described [23].

Generation and analysis of RNF170 knockout and reconstituted cell lines - The CRISPR/Cas9 system [24,25] was used to target an exon within the mouse RNF170 gene that was common to all predicted splice variants (exon 6). Oligonucleotides that contained the RNF170 target CRISPR sequence (*GATACTGGCGATACGGGTCCTGG*) were annealed and then ligated into *Afl*II-linearized gRNA vector (Addgene). αT3 mouse pituitary cells were transfected [18] with a mixture of the gRNA construct and vectors encoding Cas9 (Addgene) and EGFP (Clontech). Two days post-transfection, EGFP-expressing cells were selected by Fluorescence-Activated Cell Sorting and plated at ~1 cell per well in 96-well plates. Colonies were expanded and screened for ablation of RNF170 expression by immunoblotting with anti-RNF170 (raised against amino acids 50-65 of RNF170) [15]. Of the cell lines screened, ~30% lacked RNF170 and 2 of those were expanded for characterization of IP_3R1 processing with essentially identical results; clone IC8 was used for the experiments shown in Figure 7. Reconstituted cell lines were obtained by transfecting clone IC8 with cDNAs encoding mouse RNF170 and ^{R198C}RNF170 [18], followed by selection in 1.3 mg/ml G418 for 72h, plating at ~1 cell per well in 96-well plates, colony expansion, screening with anti-RNF170, and maintenance in 0.3mg/ml G418. 2 clones expressing each construct were characterized with essentially identical results.

For analysis of IP_3R1 ubiquitination and protein levels, cells were incubated with 1%

Downloaded from http://www.jbc.org/ at Shanghai Information Center for Life Sciences, Chinese Academy of Sciences on May 25, 2015

CHAPS lysis buffer lacking dithiothreitol, but supplemented with 5mM *N*-ethylmaleimide, for 30min at 4ºC, followed by addition of 5mM dithiothreitol and centrifugation (16,000 x g for 10min at 4ºC). Lysates were then incubated with anti-IP_3R1 to immunoprecipitate IP_3R1 as described [15] and complexes were heated at 37ºC for 30min prior to SDS-PAGE in 5% gels for ubiquitin conjugate analysis, or 100ºC for 5min prior to SDS-PAGE in 10% gels for analysis of other proteins. $[Ca^{2+}]_c$ was measured as described [23].

Data presentation – All experiments were repeated at least once, and representative images of gels or traces are shown. Immunoreactivity was detected and quantitated using Pierce ECL reagents and a GeneGnome Imager (Syngene Bio Imaging). Quantitated data are expressed as mean ± SEM or range of *n* independent experiments.

Results

Analysis of the membrane topology of RNF170 – The predicted topology of mouse RNF170, derived from bioinformatic analysis, together with the amino acid sequences of TM domains 2 and 3 are depicted in Fig 1A. The sequence of human RNF170 is very similar to that of mouse RNF170 (91% identical) and human RNF170 has the same predicted topology [15,16]. Note that R^{199} in the human sequence corresponds to R^{198} in the mouse sequence, because of the absence of D^{16} from the latter [15,16]. The existence of TM domains 2 and 3 was confirmed experimentally, using a series of truncation mutants containing a C-terminal HA/glycosylation tag that together with an assessment of sensitivity to the deglycosylating activity of endo H, can provide information on orientation across the ER membrane [22,26] (Fig 1B). That full length RNF170 (^{N267}RNF170^{HA}) is insensitive to endo H (and is therefore not glycosylated) localizes this construct's C-terminus to the cytosol (Fig 1B). In contrast, the sensitivity of ^{N230}RNF170^{HA} to endo H shows that this construct's C-terminus is glycoslyated and is within the ER lumen, demonstrating that TM2 traverses the ER membrane (Fig 1B). Following the same logic, that ^{N200}RNF170^{HA} is insensitive to endo H and is not glycosylated, localizes this construct's C-terminus to the cytosol and confirms the orientation of TM2 (Fig 1B). Finally, to confirm the location of the N-terminus, ^{G8N}RNF170^{FLAG} was created, which due to replacement of G^8 with asparagine, contains an *N*-glycosylation consensus sequence (NQS) [22,26] very near the N-terminus. This construct was partially glycosylated, indicating that the N-terminus is located in the ER lumen (Fig 1B); that the glycosylation was relatively weak may be because the consensus sequence is sub-optimal, in comparison to the optimal sequence (NSTMMS) present in the other constructs [22]. Overall, these data are consistent with the topology of TM domains 1, 2 and 3 shown in Fig 1A.

Effects of the R^{198} to C mutation on RNF170 - Remarkably, the R^{198} to C mutation significantly reduced RNF170 expression. This was seen when the mutation was introduced into either untagged RNF170 or RNF170^{FLAG} (Fig 2A). Further, the mutants migrated ~1kDa more rapidly than their wild-type counterparts (Fig 2A). Additional mutants were made to explore the basis for the reduction in expression and the migration shift, using RNF170^{FLAG} as a template (Fig 2B). To examine the possibility that these changes resulted from disulphide bond formation with the newly introduced cysteine, R^{198} was replaced with serine, which is similar in size to cysteine, but which cannot form disulphide bonds. However, ^{R198S}RNF170^{FLAG} also expressed poorly and migrated rapidly (Fig 2B, lane 3), ruling out a role for disulphide bonds. Likewise, to examine whether the changes were due to loss arginine's bulky side chain, or positive charge, R^{198} was replaced with glutamine, which is relatively bulky, but is uncharged, albeit polar. ^{R198Q}RNF170^{FLAG} also expressed quite poorly and migrated rapidly (lane 4), suggesting that it is not arginine's bulk, but rather its positive charge, that is necessary for normal expression and migration. This was confirmed by replacing R^{198} with lysine, which has a slightly shorter side chain, but is still positively charged; ^{R198K}RNF170^{FLAG} expressed and migrated similarly to ^{WT}RNF170^{FLAG} (lane 5).

Examination of the amino acid sequences of TM domains 2 and 3 (Fig 1A) revealed the presence of an additional arginine in TM2 (R^{200}) and two aspartic acids in TM3 (D^{231} and D^{232}) (Fig 1A), suggesting that ionic interactions between TM2 and TM3 could be required for wild-type behavior. Mutation of these amino acids confirmed this notion, as ^{R200C}RNF170^{FLAG}, ^{D231A}RNF170^{FLAG}, ^{D232A}RNF170^{FLAG} and

Downloaded from http://www.jbc.org/ at Shanghai Information Center for Life Sciences, Chinese Academy of Sciences on May 25, 2015

$^{D231A/D232A}$RNF170^{FLAG} all expressed poorly and migrated more rapidly than RNF170^{FLAG} (lanes 6-9). Thus, ionic interactions between arginines in TM2 and aspartic acids in TM3 appear to be required for normal expression of RNF170. Further, it appears that 2 charged amino acids in each TM are required for normal expression, since mutation one arginine and one aspartic acid in $^{R198C/D231A}$RNF170^{FLAG} did not rescue expression (lane 10). Finally, it is noteworthy that accelerated migration correlated well with reduced expression (Fig 2B) and was caused by both arginine and aspartic acid loss and is therefore not due to a change in net protein charge. Rather, these data, together with the fact that RNF170 migrates at 21.5kDa rather than the predicted 30kDa [15], suggest that RNF170 is not fully denatured during SDS-PAGE and that the mutations affect the structural organization that is retained. The mutations may also alter the structure of RNF170 *in vivo*, which in turn, could account for the reductions in expression, perhaps because of protein destabilization.

Mechanism of reduced expression – To explore possible destabilization mechanisms, we examined the effects of the proteasome inhibitor MG-132. When incubated with cells expressing exogenous RNF170^{FLAG} constructs (Fig 3A), MG-132 caused a marked accumulation of ^{R198C}RNF170^{FLAG} (lanes 4-6), while leaving ^{WT}RNF170^{FLAG} levels essentially unaltered (lanes 1-3). Thus, the proteasome appears to mediate the reduced expression of ^{R198C}RNF170^{FLAG}. Further, as E3 autoubiquitination is a commonly observed phenomenon [27], we examined the effects of inactivating ligase activity on ^{R198C}RNF170^{FLAG} expression. Previously, we have shown that mutation of C^{101} and H^{103} in the RING domain of mouse RNF170 blocks ubiquitin ligase activity [15], and introduction of these mutations into ^{R198C}RNF170^{FLAG} (creating $^{R198C/\Delta RING}$RNF170^{FLAG}) normalized expression (Fig 3B, lane 4), suggesting that ligase activity, and most likely autoubiquitination, mediates the reduced expression of ^{R198C}RNF170^{FLAG}. Interestingly, the $^{R198C/\Delta RING}$RNF170^{FLAG} mutant still migrated faster than ^{WT}RNF170^{FLAG}, suggesting that the putative structural change has not been reversed by mutation of the RING domain (Fig 3B, lane 4). A role for autoubiquitination was supported by the observation that ^{WT}RNF170^{HA} expression was not differentially affected by co-expression of ^{WT}RNF170^{FLAG} and ^{R198C}RNF170^{FLAG} (Fig 3C, lanes 2 and 3); this result shows that the apparent destabilizing effect of the R198C mutation is intramolecular and is not transmitted to co-expressed ^{WT}RNF170^{HA} molecules. Importantly, ^{R198C}RNF170^{FLAG} exhibited *in vitro* ubiquitin ligase activity similar to that of ^{WT}RNF170^{FLAG} (Fig 3D, lanes 2 and 4), indicating that it is fully capable of autoubiquitinating. Finally, to determine protein half-lives, transfected cells were incubated with the protein synthesis inhibitor CHX (Fig 3E). This revealed that the half-life of ^{R198C}RNF170^{FLAG} is much shorter than that of ^{WT}RNF170^{FLAG}, and that MG-132 blocks ^{R198C}RNF170^{FLAG} degradation. Overall, these data indicate that the R198C mutation decreases RNF170 expression by triggering the molecule to autoubiquitinate and then be degraded by the proteasome.

The R198C mutation does not alter membrane topology, subcellular localization, or interaction with the erlin1/2 complex – To explore why mutation-induced salt bridge disruption triggers RNF170 autoubiquitination, we first examined whether subcellular localization was altered. However, the extent of *N*-glycosylation seen for the relevant constructs shown in Fig 1B (^{N267}RNF170^{HA} and ^{N230}RNF170^{HA}) was not substantially altered by introduction of the R198C mutation (Fig 4A), indicating that localization to the ER and insertion of TM domains is normal. Likewise, interaction with the endogenous erlin1/2 complex was normal, since immunoprecipitation with anti-erlin2 [15] recovered ^{WT}RNF170^{HA} and ^{R198C}RNF170^{HA} equally well (Fig 4B). Further, membrane association was normal, as both ^{WT}RNF170^{HA} and ^{R198C}RNF170^{HA} fractionated with membranes (Fig 4C). Thus, the R198C mutation does not dramatically alter the localization of RNF170, indicating that a subtle change in its properties (e.g. in the way that it folds) accounts for its apparent autoubiquitination and proteasomal degradation.

RNF170 expression in control and ADSA affected individuals – Lymphoblast lines from control and ADSA affected individuals were examined for RNF170 expression (Fig 5A). In controls, an anti-RNF170 immunoreactive band at ~21.5kDa was observed (lanes 1-3), the same size as endogenous HeLa cell RNF170 and untagged mouse RNF170 (Fig 2A). Remarkably, in affected lymphoblasts

Downloaded from http://www.jbc.org/ at Shanghai Information Center for Life Sciences, Chinese Academy of Sciences on May 25, 2015

the strength of the 21.5kDa band was reduced and an additional weaker band at ~20.5kDa was also observed (lanes 4-6). These results are consistent with the expression level and migration differences seen between exogenous mouse ^{WT}RNF170 and ^{R198C}RNF170 (Fig 2A) and between exogenous human ^{WT}RNF170 and ^{R199C}RNF170 (Fig 5B), and with the knowledge that affected individuals are heterozygote [16]. Thus, it appears that the ^{R199C}RNF170 encoded by the mutant allele in affected individuals migrates at ~20.5kDa and is relatively poorly expressed. This leads to an ~27% reduction in total RNF170 immunoreactivity in affected lymphoblasts (Fig 5A).

Ca^{2+} mobilization via IP_3 receptors is impaired in affected lymphoblasts - Because IP_3Rs are the only known substrates for RNF170 [15], we examined whether IP_3R function was different in control and affected lymphoblasts, using PAF to trigger IP_3R-mediated Ca^{2+} mobilization [28] (Fig 6). Remarkably, PAF-induced increases in $[Ca^{2+}]_c$ were significantly suppressed in affected lymphoblasts (Fig 6A), suggesting that IP_3R-mediated Ca^{2+} mobilization might be impaired, although the suppression could also be due to an effect on Ca^{2+} entry [29]. To rule out any role for Ca^{2+} entry, EGTA was added immediately prior to PAF to chelate extracellular Ca^{2+} to ~ 100 nM [23], and under these conditions the suppression of PAF-induced increases in $[Ca^{2+}]_c$ was still clearly evident (Fig 6B). To examine if the suppression results from ER Ca^{2+} stores being smaller, cells were exposed to the SERCA pump inhibitor thapsigargin, which allows Ca^{2+} leak from the ER in an IP_3R-independent manner [30]. However, thapsigargin caused the same $[Ca^{2+}]_c$ increase in control and affected lymphoblasts (Fig 6C), indicating that Ca^{2+} stores are of equal size. Likewise, reduced IP_3 formation was not the reason for the suppression, as PAF-induced increases in IP_3 mass were the same in control and affected lymphoblasts (increases over basal resulting from 0.5min exposure to 100nM PAF were 24 ± 8% and 35 ± 15 %, respectively; n=3). Finally, measurement of the levels of IP_3R1-3 did not reveal any consistent differences between control and affected lymphoblasts (Fig 6D). Overall, these data indicate that Ca^{2+} mobilization via IP_3Rs is impaired in affected lymphoblasts, but not because of a change in Ca^{2+} store size, or the abundance of IP_3Rs, and point towards a mechanism that involves a regulation of IP_3R activity.

Ubiquitin ligase activity of RNF170 and ^{R198C}RNF170 in cells - ^{R198C}RNF170 exhibits apparently normal ubiquitin ligase activity *in vitro* when mixed with purified enzymes (Fig 3D), but that tells us almost nothing about how its activity might differ from that of ^{WT}RNF170 *in vivo*, where the intracellular milieu contains a full complement of E2s, substrates and other factors. To date, endogenous activated IP_3Rs are the only known substrates for RNF170 [15], but it has yet to be resolved whether RNF170 is responsible for the addition of all of the ubiquitin conjugates that become attached to activated IP_3Rs, or just some [17,18]. Initially, we sought to compare the ligase activities of ^{WT}RNF170 and ^{R199C}RNF170 towards IP_3Rs in control and ADSA lymphoblasts, but pilot experiments showed that to be unfeasible, primarily because of the paucity of IP_3Rs therein (data not shown). Thus, we employed αT3 cells, the cells in which we first identified RNF170 [15] and which exhibit very robust IP_3R1 ubiquitination in response to the IP_3-generating, cell surface receptor agonist GnRH [17,18]. First, to determine which ubiquitin conjugates RNF170 adds, we deleted RNF170 using CRISPR/Cas9-mediated gene editing (Fig 7). RNF170 "knock-out" was specific (Fig 7A), as other pertinent proteins (e.g. the ERAD pathway proteins p97, Hrd1 and gp78 [6,7] and erlins 1 and 2) were expressed at the same level in control and "αT3 RNF170KO" cells. Interestingly, IP_3R1 expression was enhanced ~65% by RNF170 deletion (Fig 7A and D), indicating that in addition to its role in mediating the degradation of activated IP_3Rs [15], RNF170 also plays a role in basal IP_3R1 turnover. Ca^{2+} mobilization in αT3 RNF170KO cells in response to GnRH was normal (Fig 7B), indicating that the IP_3-dependent signaling pathway and IP_3R activation is not perturbed by the absence of RNF170. Remarkably, deletion of RNF170 completely blocks GnRH-induced IP_3R1 ubiquitination (Fig 7C), observed using either FK2 antibody which detects all ubiquitin conjugates (monoubiquitin, and Lys-48- and Lys-63-linked chains), or antibodies specific for Lys-48- and Lys-63-linked chains [18]. In contrast, erlin2 association with IP_3R1 was not blocked, indicating that association

Downloaded from http://www.jbc.org/ at Shanghai Information Center for Life Sciences, Chinese Academy of Sciences on May 25, 2015

of the erlin1/2 complex with activated IP_3R1 is unimpaired, consistent with the notion that it is the erlin1/2 complex that recruits RNF170 to activated IP_3R1, rather than vice-versa [12,15]. Thus, RNF170 does indeed catalyze the formation of all ubiquitin conjugates on activated IP_3R1, and as would be expected, GnRH did not cause IP_3R down-regulation in αT3 RNF170KO cells (Fig 7D).

To directly assess the ligase activity of ^{R198C}RNF170, we sought to reconstitute IP_3R ubiquitination in αT3 RNF170KO cells by stably expressing exogenous RNF170 constructs (Fig 7E). Cell lines were obtained, although exogenous expression was less than that seen for endogenous RNF170 in control αT3 cells (data not shown). Both ^{WT}RNF170 and ^{R198C}RNF170 were capable of ubiquitinating activated IP_3Rs, as indicated by increases in Lys-48- and Lys-63-linked ubiquitin chains and total ubiquitin after exposure to GnRH (Fig 7E). That less ubiquitination was seen in ^{R198C}RNF170-expressing cells is most likely a consequence of lower expression level and IP_3R binding of the mutant (Fig 7E). Thus, the ligase activity of ^{R198C}RNF170 towards IP_3Rs receptors *in vivo* appears to be qualitatively normal, and aberrant IP_3R receptor ubiquitination is unlikely to account for the Ca^{2+} signaling deficit seen in ADSA lymphoblasts.

Discussion

Our data show that the R^{198} to C mutation in mouse RNF170 reduces the stability and expression level of the protein. The mutation appears to disrupt a salt bridge between TM domains 2 and 3 and leads to autoubiquitination and enhanced turnover via the ubiquitin-proteasome pathway. This mechanism also likely applies to human ^{R199C}RNF170 in ADSA affected individuals, and accounts for the ~27% reduction in the total cellular complement of RNF170. An equivalent decrease in cellular ligase activity attributable to RNF170 is likely, which could be critical to development of the disease. Alternatively, the ligase activity of mutant RNF170 *in vivo* could be abnormal. We did not obtain support for this notion from studies with purified components *in vitro* (Fig 3D), or from analysis of IP_3R1 ubiquitination *in vivo* (Fig 7E), but that does not rule out the possibility that mutant RNF170 acts abnormally towards other substrates. Mutant RNF170 acting in this manner (i.e. dominantly) would be consistent with zebrafish studies, in which expression of exogenous mutant RNF170 causes aberrant development [16].

Prior to the current study, our approach to defining the function of RNF170 (and other proteins suspected to play a role in IP_3R ERAD) has been to deplete them using RNA interference. While we have had some success with this approach [13-15,31] it has major limitations; in particular, proteins are only *depleted* and the effects of residual proteins are hard to assess and complicate interpretation of data from reconstitution experiments, and cells expressing short interfering RNA are often unhealthy and are available only in limited quantities. Use of the CRISPR/Cas9 system [24,25] allowed us to *delete* RNF170 and demonstrate, for the first time, that RNF170 catalyzes the addition of all ubiquitin conjugates to activated IP_3R1. Intriguingly, this suggests that RNF170 interacts with multiple E2s, most likely Ubc13 and Ubc7, since Ubc13 is the only E2 known to build K63-linked chains [5,32] and Ubc7, which builds K48-linked chains [5,32], is already strongly implicated in mediating IP_3R1 ubiquitination and degradation [33].

Why does the R^{198} to C mutation destabilize RNF170? It appears that a network of salt bridges couple TM domains 2 and 3 together, since mutation of either R^{198} or R^{200} in TM2 reduces protein expression, as do mutations to D^{231} and D^{232} in TM3. A hint as to why these mutations are apparently destabilizing is provided by the fact that they also cause RNF170 to migrate more rapidly on SDS-PAGE, indicative of a structural change in the protein that either causes more compact folding and / or alters interactions with SDS. The structural change appears to be subtle, as the R^{198} to C mutation did not significantly affect TM2 and TM3 insertion into the ER membrane, or interaction with the erlin1/2 complex, but could still be sufficient to trigger autoubiquitination and targeting for ERAD. Interestingly, many other E3s are known to be regulated by ubiquitination [3,27], including the ER membrane ligase gp78 [27], which is relatively unstable and is controlled both by autoubiquitination and by an additional ER membrane ubiquitin ligase Hrd1 [27]. It will be interesting to see whether mutations in the TM

Downloaded from http://www.jbc.org/ at Shanghai Information Center for Life Sciences, Chinese Academy of Sciences on May 25, 2015

domains of gp78 and other ER membrane ligases [8] are also destabilizing.

While the presence of charged residues in TM domains is energetically unfavorable, such residues are often found therein, where they play important functions, often involving salt bridges [34]. Intriguingly, TM domain-located charged residues are those most likely to cause disease when mutated, arginine has the highest propensity for disease causation, and the R to C mutation is relatively common because cytosine to thymine transition occurs with relatively high frequency [35]. Situations very similar to that described here for RNF170 are seen in other proteins. For example, the pore architecture of cystic fibrosis transmembrane conductance regulator is maintained by salt bridges between arginines in TM6 (R347 and R352) and aspartic acids in adjacent TMs [36], and naturally occurring, charge altering mutations of R352 cause cystic fibrosis [37]. Likewise, the naturally occurring R279C mutation in the prostacyclin receptor dramatically reduces protein expression [38].

Remarkably, the expression of ^{R199C}RNF170 correlated with a reduction in PAF-induced Ca^{2+} mobilization in lymphoblasts that was not due to a change in IP_3R levels, but rather appears to result from reduced signal transduction efficiency at the IP_3R locus. This was apparently not due to aberrant IP_3R ubiquitination, as the ubiquitination of activated IP_3R1 in cells expressing wild-type or mutant RNF170 was qualitatively identical, at least in terms of the addition of total ubiquitin and Lys-48- and Lys-63-linked chains. Rather, the reduction in signal transduction efficiency at the IP_3R locus could be an indirect effect, if RNF170 turns out to ubiquitinate additional substrates (e.g. proteins that regulate IP_3Rs), or if long-term adaptation to the ~27% reduction in total RNF170 expression seen in ADSA lymphoblasts alters the expression of genes that govern Ca^{2+} signaling.

Dysregulation of Ca^{2+} metabolism and IP_3R function is often mooted to be the cause of the neurodegeneration that underpins certain spinocerebellar ataxias and neurodegenerative diseases [39-43] and our data suggest that the same could be true for ADSA. If so, therapies aimed at boosting Ca^{2+} mobilization could be contemplated, similarly to the way that manipulating Ca^{2+} metabolism is being examined as a therapy for Huntington's disease and other spinocerebellar ataxias [41-43]. Interestingly, mutations to erlin2 also cause neurodegenerative diseases [44-47]. Erlin2 is the dominant partner in the erlin1/2 complex, to which RNF170 is constitutively associated [11,12,15], and the erlin1/2 complex mediates the interaction of RNF170 with IP_3Rs [15]. Clearly, defining the mechanisms by which mutations to the erlin1/2 complex-RNF170 axis cause neurodegeneration will be fascinating topics for future study.

REFERENCES

1. Finley, D. (2009) Recognition and processing of ubiquitin-protein conjugates by the proteasome. *Annu. Rev. Biochem.* **78**, 477-513.
2. Kleiger, G. and Mayor, T. (2014) Perilous journey: a tour of the ubiquitin-proteasome system. *Trends Cell Biol*. **24**, 352-359.
3. Deshaies, R.J. and Joazeiro, C.A.P. (2009) RING Domain E3 ubiquitin ligases. *Annu. Rev. Biochem*. **78**, 399-434.
4. Budhidarmo, R., Nakatani, Y. and Day, C.L. (2011) RINGs hold the key to ubiquitin transfer. *Trends Biochem. Sci*. **37**, 58-65.
5. Metzger, M.B., Pruneda, J.N., Klevit, R.E. and Weissman, A.M. (2014) RING-type E3 ligases: Master manipulators of E2 ubiquitin-conjugating enzymes and ubiquitination. *Biochim. Biophys. Acta* **1843**, 47-60.
6. Ruggiano, A., Foresti, O. and Carvalho, P. (2014) ER-associated degradation: protein quality control and beyond. *J. Cell Biol.* **204**, 869-879.
7. Christianson, J.C. and Ye, Y. (2014) Cleaning up in the endoplasmic reticulum: ubiquitin in charge. *Nature Struct. Mol. Biol.* **4**, 325-335.
8. Neutzner, A., Neutzner, M., Benischke, A-S., Ryu, S-W., Frank, S., Youle, R.J. and Karbowski, M. (2011) A systematic search for endoplasmic reticulum (ER) membrane-associated RING finger

Downloaded from http://www.jbc.org/ at Shanghai Information Center for Life Sciences, Chinese Academy of Sciences on May 25, 2015

proteins identifies Nixin/ZNRF4 as a regulator of calnexin stability and ER homeostasis. *J. Biol. Chem*. **286**, 8633-8643.
9. Foskett, J. K., White, C., Cheung, K. H. and Mak, D. D. (2007) Inositol trisphosphate receptor Ca^{2+} release channels. *Physiol. Rev*. **87**, 593-658.
10. Seo, M.D., Velamakanni, S., Ishiyama, N., Stathopulos, P.B., Rossi, A.M., Khan, S.A., Dale, P., Li, C., Ames, J.B., Ikura, M. and Taylor, C.W. (2012) Structural and functional conservation of key domains in $InsP_3$ and ryanodine receptors. *Nature* **483**, 108-112.
11. Wojcikiewicz, R.J.H., Pearce, M.M.P., Sliter, D.A. and Wang, Y. (2009) When worlds collide: IP_3 receptors and the ERAD pathway. *Cell Calcium* **46**, 147-153.
12. Wojcikiewicz, R.J.H. (2012) Inositol 1,4,5-trisphosphate receptor degradation pathways. *WIREs Membr. Transp. Signal.* **1**, 126-135.
13. Pearce, M. M. P., Wang, Y., Kelley, G. G. and Wojcikiewicz, R. J. H. (2007) SPFH2 mediates the endoplasmic reticulum-associated degradation of inositol 1,4,5-trisphosphate receptors and other substrates in mammalian cells. *J. Biol. Chem.* **282,** 20104-20115.
14. Pearce, M. M. P., Wormer, D. B., Wilkens, S. and Wojcikiewicz, R. J. H. (2009) An endoplasmic reticulum (ER) membrane complex composed of SPFH1 and SPFH2 mediates the ER-associated degradation of inositol 1,4,5-trisphosphate receptors. *J. Biol. Chem.* **284,** 10433-10445.
15. Lu, J.P., Wang, Y., Sliter, D.A., Pearce, M. M. P. and Wojcikiewicz, R. J. H. (2011) RNF170, an endoplasmic reticulum membrane ubiquitin ligase, mediates inositol 1,4,5-trisphosphate receptor ubiquitination and degradation. *J. Biol. Chem.* **286,** 24426-24433.
16. Valdmanis, P.N., Dupré, N., Lachance, M., Stochmanski, S.J., Belzil, V.V., Dion, P.A., Thiffault, I., Brais, B., Weston, L., Saint-Amant, L., Samuels, M.E. and Rouleau, G.A. (2011) A mutation in the RNF170 gene causes autosomal dominant sensory ataxia. *Brain* **134,** 602-607.
17. Sliter, D., Kirkpatrick, D.S., Alzayady, K., Kubota, K., Gygi, S.P. and Wojcikiewicz, R.J.H. (2008) Mass spectral analysis of type I inositol 1,4,5-trisphosphate receptor ubiquitination. *J. Biol. Chem.* **283**, 35319-35328.
18. Sliter D.A., Aguiar, M., Gygi, S.P. and Wojcikiewicz, R.J.H. (2011) Activated inositol 1,4,5-trisphosphate receptors are modified by homogeneous LYS48- and LYS63-linked ubiquitin chains, but only LYS48-linked chains are required for degradation. *J. Biol. Chem.* **286**, 1074-1082.
19. Moeller, J.J., Macaulay, R.J.B., Valdmanis, P.N., Weston, L., Rouleau, G.A. and Dupré, N. (2008) Autosomal dominant sensory ataxia: a neuroaxonal dystrophy. *Acta Neuropathol.* **116,** 331-336.
20. Wojcikiewicz, R.J.H. (1995) Type I, II and III inositol 1,4,5 trisphosphate receptors are unequally susceptible to down-regulation and are expressed in markedly different proportions in different cell types. *J. Biol. Chem.* **270**, 11678-11683.
21. Bultynck, G., Szlufcik, K., Kasri, N.N., Assefa, Z., Callewaert, G., Missiaen, L., Parys, J.B. and De Smedt, H. (2004) Thimerosal stimulates Ca^{2+} flux through inositol 1,4,5-trisphosphate receptor type 1, but not type 3, via modulation of an isoform-specific Ca^{2+}-dependent intramolecular interaction. *Biochem. J.* **381**, 87-96.
22. Bano-Polo, M., Baldin, F., Tamborero, S., Marti-Renom, M.A. and Mingarro, I. (2011) *N*-glycosylation efficiency is determined by the distance to the C-terminus and the amino acid preceding an Asn-Ser-Thr sequon. *Protein Sci.* **20,** 179-186.
23. Wojcikiewicz, R.J.H., Tobin, A.B. and Nahorski, S.R. (1994) Muscarinic receptor-mediated inositol 1,4,5-trisphosphate formation in SH-SY5Y neuroblastoma cells is regulated acutely by cytosolic Ca^{2+} and by rapid desensitization. *J. Neurochem.* **63,** 177-185.
24. Mali, P., Yang, L., Esvelt, K.M., Aach, J., Guell, M., DiCarlo, J.E., Norville, J.E. and Church, G.M. (2013) RNA-guided human genome engineering via Cas9. *Science* **339**, 823-826.
25. Ran, F.A., Hsu, P.D., Wright, J., Agarwala, V., Scott, D.A. and Zhang, F. (2013) Genome engineering using the CRISPR-Cas9 system. *Nat. Protoc.* **8**, 2281-2308.
26. Van Geest, M. and Lolkema, J.S. (2000) Membrane topology and insertion of membrane proteins: search for topogenic signals. *Microbiol. Mol. Biol. Rev*. **64**, 13-33.

Downloaded from http://www.jbc.org/ at Shanghai Information Center for Life Sciences, Chinese Academy of Sciences on May 25, 2015

27. Weissman, A.M., Shabek, N. and Ciechanover, A. (2011) The predator becomes the prey: regulating the ubiquitin system by ubiquitylation and degradation. *Nat. Rev. Mol. Cell Biol.* **12**, 605-620.
28. Pietruck, F., Spleiter, S., Daul, A., Philipp, T., Derwahl, M., Schatz, H. and Siffert, W. (1998) Enhanced G protein activation in IDDM patients with diabetic nephropathy. *Diabetologica* **41**, 94-100.
29. Rosskopf, D., Daelman, W., Busch, S., Schurks, M., Hartung, K., Kribben, A., Michel, M.C. and Siffert, W. (1998) Growth factor-like action of lysophosphatidic acid on human B lymphoblasts. *Am. J. Physiol.* **274**, C1573-1582.
30. Thastrup, O., Cullen, P.J., Drobak, B.K., Hanley, M.R. and Dawson, A.P. (1990) Thapsigargin, a tumour promoter, discharges intracellular Ca2+ stores by specific inhibition of the endoplasmic reticulum Ca2+-ATPase. *Proc. Natl. Acad. Sci. USA*. **87,** 2466-2470.
31. Alzayady, K.J., Panning, M.M., Kelley, G.G. and Wojcikiewicz, R.J.H. (2005) Involvement of the p97-Ufd1-Npl4 Complex in the Regulated Endoplasmic Reticulum-associated Degradation of Inositol 1,4,5-Trisphosphate Receptors. *J. Biol. Chem*. **280**, 34530-34537.
32. Ye, Y. and Rape, M. (2009) Building ubiquitin chains: E2 enzymes at work. *Nature Rev. Mol. Cell Biol*. **10**, 755-764.
33. Webster, J.M., Tiwari, S., Weissman, A.M. and Wojcikiewicz, R.J.H. (2003) Inositol 1,4,5 trisphosphate receptor ubiquitination is mediated by mammalian Ubc7, a component of the Endoplasmic Reticulum-Associated Degradation pathway, and is inhibited by chelation of intracellular Zn^{2+}. *J. Biol. Chem.* **278**, 38238-38246.
34. Von Heijne, G. (2006) Membrane-protein topology. *Nat. Rev. Mol. Cell Biol*. **7**, 909-918.
35. Partridge, A.W., Therien, A.G. and Deber, C.M. (2004) Missense mutations in transmembrane domains of proteins: phenotypic propensity of polar residues for human disease. *Proteins* **54**, 648-656.
36. Cui, G., Freeman, C.S., Knotts, T., Prince, C.Z., Kuang, C. and McCarty, N.A. (2013) Two salt bridges differentially contribute to the maintenance of cystic fibrosis conductance regulator (CFTR) channel function. *J. Biol. Chem.* **288**, 20758-20767.
37. Cui, G., Zhang, Z-R., O'Brien, A.R.W., Song, B. and McCarty, N.A. (2008) Mutations at arginine 352 alter the pore architecture of CFTR. *J. Membr. Biol.* **222**, 91-106.
38. Stitham, J., Arehart, E., Gleim, S.R., Li, N., Douville, K. and Hwa, J. (2007) New insights into human prostacyclin receptor structure and function through natural and synthetic mutations of transmembrane charged residues. *Brit. J. Pharmacol*. **152**, 513-522.
39. Paulson, H.L. (2009) The spinocerebellar ataxias *J. Neuroopthamol*. **29**, 227-237.
40. Matilla-Duenas, A., Corral-Juan, M., Volpini, V. and Sanchez, I. (2012) The spinocerebellar ataxias: clinical aspects and molecular genetics. *Adv. Exp. Med. Biol.* **724**, 351-374.
41. Bezprozvanny, I. (2011) Role of inositol 1,4,5-trisphosphate receptors in pathogenesis of Huntington's disease and spinocerebellar ataxias. *Neurochem. Res.* **36**, 1186-1197.
42. Foskett, J.K. (2010) Inositol trisphosphate receptor Ca2+ release channels in neurological diseases. *Pfugers Arch.* **460**, 481-494.
43. Brown, S-A. and Loew, L.M. (2015) Integration of modeling with experimental and clinical findings synthesizes and refines the central role of inositol 1,4,5-trisphosphate receptor 1 in spinocerebellar ataxia. *Front. Neurosci.* **8**, 453.
44. Yildirim, Y., Orhan, E.K., Iseri, S.A., Serdaroglu-Oflazer, P., Kara, B., Solakoglu, S. and Tolun, A. (2011) A frameshift mutation of erlin2 in recessive intellectual disability, motor dysfunction and multiple joint contractures. *Hum. Mol. Genet*. **20**, 1886-1892.
45. Alazami, A.M., Adly, N., Al Dhalaan, H. and Alkuraya, F.S. (2011) A nullimorphiic *erlin2* mutation defines a complicated hereditary spastic paraplegia locus (SPG18). *Neurogenetics* **12**, 333-336.
46. Al-Saif, A., Bohlega, S. and Al-Mohanna, F. (2012) Loss of erlin2 function leads to juvenile primary lateral sclerosis. *Ann. Neurol.* **72**, 510-516.

Downloaded from http://www.jbc.org/ at Shanghai Information Center for Life Sciences, Chinese Academy of Sciences on May 25, 2015

47. Wakil, S.M., Bohlega, S., Hagos, S., Baz, B., Al Dossari, H., Ramzan, K. and Al-Hassnan, Z.N. (2013) A novel splice site mutation in erlin2 causes hereditary spastic paraplegia in a Saudi family. *Eur. J. Med. Genet*. **56**, 43-45.

FOOTNOTES

The authors thank Erik Vandermark and Jacqualyn Schulman for helpful suggestions and National Institutes of Health Grant DK049194 and the National Ataxia Foundation for financial support.

The abbreviations used are: IP_3, inositol 1,4,5-trisphosphate; IP_3R, inositol 1,4,5-trisphosphate receptor; ER, endoplasmic reticulum; ERAD, ER-associated degradation; ADSA, autosomal dominant sensory ataxia; TM, transmembrane; E3, ubiquitin ligase; E2, ubiquitin-conjugating enzyme; PAF, platelet activating factor; GnRH, gonadotropin-releasing hormone; CHX, cycloheximide; $[Ca^{2+}]_c$, cytosolic Ca^{2+} concentration.

FIGURE LEGENDS

Figure 1. Membrane topology of RNF170.
A. Predicted topology of RNF170 [15] with the TM2/3 region expanded to show the mouse amino acid sequence. Note that the amino acid that corresponds to R^{199} of human RNF170 is R^{198} in mouse RNF170, and that the sequences of human and mouse TM2/3 regions are identical, with the exception that M^{202} of mouse RNF170 is I^{203} in human RNF170 [15,16]. The RING domain, the three TM domain regions and the N and C termini are indicated, and R^{198} is identified with an asterisk. The precise limits of the predicted TM domains have not been defined experimentally, but the scheme shown is predicted by multiple programs (e.g. TMHMM, TOPCONS, etc). B. *N*-Glycosylation of RNF170 mutants. An HA/glycosylation tag (black box) was introduced at the C-terminus of full length RNF170 (^{N267}RNF170^{HA}), or truncated RNF170 lacking putative TM domain 3 (^{N230}RNF170^{HA}), or putative TM domains 2 and 3 (^{N200}RNF170^{HA}). These, and ^{G8N}RNF170^{FLAG} (FLAG tag indicated by a grey box and the G8N mutation with a circle) were expressed in HeLa cells, lysates were incubated without or with 1U/µl endo H for 3h at 37°C, and samples were subjected to SDS-PAGE. Blots were then probed with anti-HA or anti-FLAG to identify the exogenous RNF170 constructs, or anti-erlin2 to identify endogenous erlin2, which is known to be *N*-glycosylated [13,14], and which serves as a positive control for endo H. The migration positions of unmodified and *N*-glycosylated species are indicated with arrows and arrowheads, respectively; degylcosylation of erlin2, ^{N230}RNF170^{HA} and ^{G8N}RNF170^{FLAG} by endo H reduces their apparent molecular masses by ~2kDa.

Figure 2. Effects of mutation of R^{198} and other amino acids on RNF170 expression
cDNAs encoding wild-type (WT) and mutant RNF170 constructs and vector alone were transfected into HeLa cells and cell lysates were probed as indicated. Erlin2 and β-tubulin served as loading controls. A. Lysates were probed with anti-RNF170, which detects both endogenous and exogenous untagged RNF170 constructs (lanes 1-5), or with anti-FLAG, which detects just exogenous FLAG-tagged constructs (lanes 6-10). B. Lysates were probed with anti-FLAG and the histogram shows combined quantitated immunoreactivity (mean±SEM, $n \geq 3$).

Figure 3. The R198C mutation reduces RNF170 expression via autoubiquitination and the proteasome
A-C. cDNAs encoding tagged WT and mutant RNF170 constructs were transfected into HeLa cells, were treated as indicated, and cell lysates were probed with anti-FLAG or anti-HA to recognize exogenous RNF170 constructs, or anti-erlin2, which served a loading control. The histograms show combined quantitated immunoreactivity (mean±SEM, $n \geq 4$). D. RNF170^{FLAG} constructs were immunopurified from transfected HeLa cells and were incubated with E1 (*UBE1*), E2 (*UbcH5b*) and HA-ubiquitin as indicated for 30min at 30°C, with the exception of lane 1, which lacked E2. Samples were then probed

Downloaded from http://www.jbc.org/ at Shanghai Information Center for Life Sciences, Chinese Academy of Sciences on May 25, 2015

with anti-HA to assess ubiquitination (upper panel), or anti-FLAG to assess the levels of $RNF170^{FLAG}$ constructs (lower panel). The asterisk marks a background band. E. Transfected HeLa cells were treated as indicated with 20μg/ml CHX, without or with 10μM MG-132. Cell lysates were then probed with anti-p53 as a positive control for CHX action, anti-p97 as a loading control, and anti-FLAG to recognize exogenous RNF170 constructs (long and short exposures are shown to facilitate visualization of immunoreactivity changes). The graph shows combined quantitated FLAG immunoreactivity, using the long exposure for $^{R198C}RNF170^{FLAG}$ and the short exposure for $^{WT}RNF170^{FLAG}$ (mean±range, n = 2).

Figure 4. Lack of effect of the R198C mutation on RNF170 membrane association and topology, and interaction with the erlin1/2 complex

cDNAs encoding HA-tagged WT and mutant RNF170 constructs were transfected into HeLa cells. A. *N*-Glycosylation of $^{N267/R198C}RNF170^{HA}$ and $^{N230/R198C}RNF170^{HA}$, R198C-containing versions of the constructs shown in Fig 1B, was assessed as in Fig 1B. B. Interaction with the erlin1/2 complex. Erlin1/2 complex was immunoprecipitated with anti-erlin2 was probed for RNF170 constructs (lower panels). Note that the amounts of $^{WT}RNF170^{HA}$ and $^{R198C}RNF170^{HA}$ that co-immunoprecipitate are proportional to the amounts in input lysates, indicating that they interact with the erlin1/2 complex equally well. C. Cells were lysed and centrifuged into cytosol (C) and membrane (M) factions as described [13], and were probed as indicated.

Figure 5. RNF170 levels in lymphoblasts from control and ADSA affected individuals

A. Lysates from 3 control (lanes 1-3) and 3 affected individuals (lanes 4-6) were probed with anti-RNF170 and anti-erlin2. For the panels shown, immunoreactivity was quantitated and is plotted as total RNF170/erlin2 immunoreactivity (arbitrary units). Multiple quantitations of total RNF170 immunoreactivity from these and other lymphoblast lines showed that affected individuals contained 73 ± 5 % of the immunoreactivity seen in control lymphoblasts ($n \geq 5$). B. cDNAs encoding human $^{WT}RNF170^{HA}$ and $^{R199C}RNF170^{HA}$ were transfected into HeLa cells and cell lysates were probed as indicated. Erlin2 and served as a loading control.

Figure 6. Assessment of the IP_3-medited Ca^{2+} signaling pathway in lymphoblasts

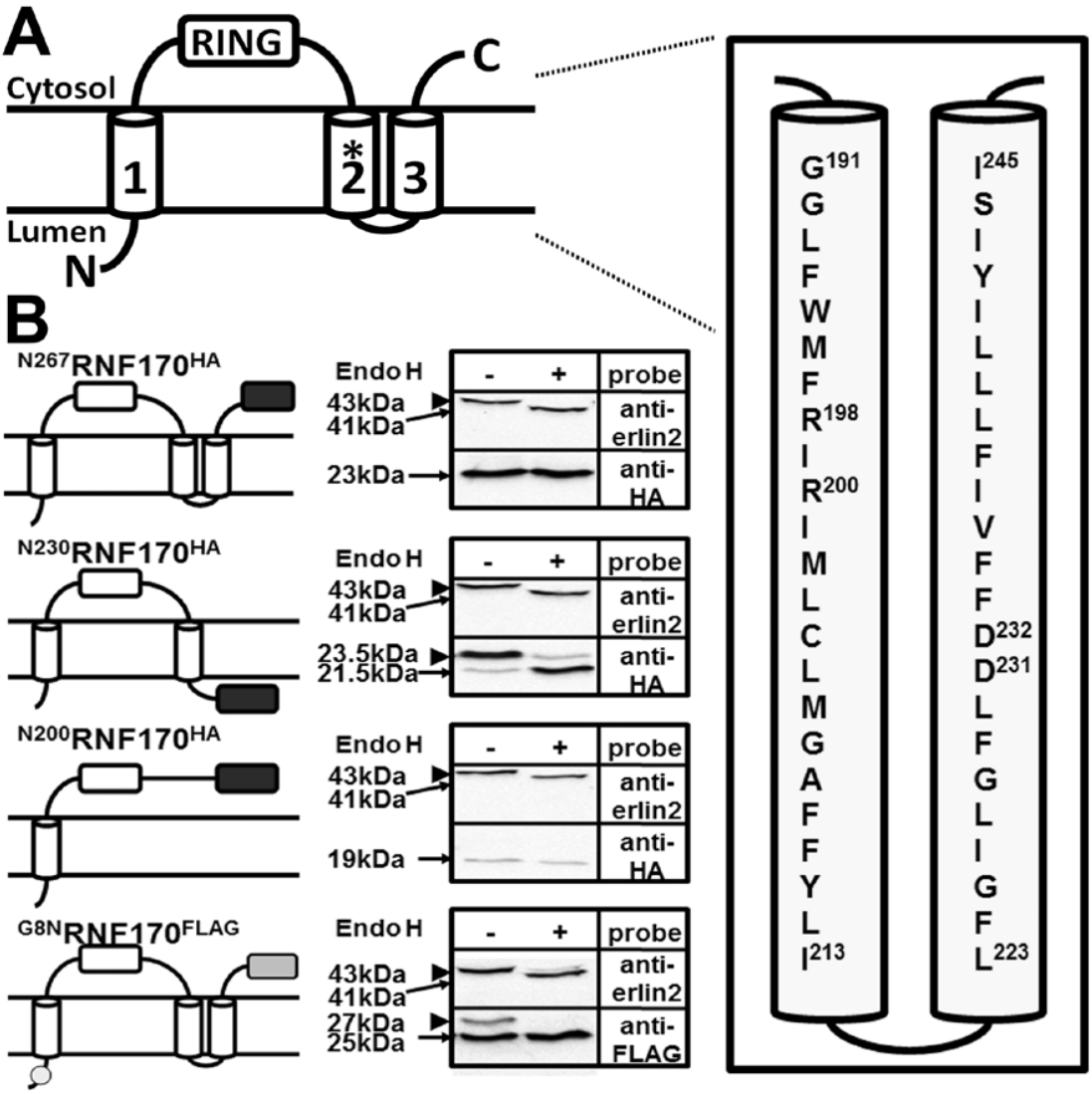
Multiple control and affected lymphoblast cell lines (n) were analyzed. A-C. Fura2-loaded cells were exposed to PAF, EGTA and thapsigargin (TG) as indicated and $[Ca^{2+}]_c$ was calculated. Values in parentheses are mean ± SEM of PAF- or TG-induced increases in $[Ca^{2+}]_c$ over basal values ($n \geq 4$, with * indicating $p < 0.05$ when comparing values from control versus affected cells). D. Lysates from 4 control and 4 affected lymphoblast lines were probed for the proteins indicated. Total IP_3R immunoreactivity in control and affected lymphoblasts, measured with anti-IP_3R1-3 (lowest panel), was 80±20 and 76±15 arbitrary units, respectively (mean±SEM).

Figure 7. CRISPR/Cas9-mediated deletion of RNF170 and reconstitution with exogenous RNF170 constructs

A. Levels of RNF170, IP_3R1 and other pertinent proteins in lysates from αT3 control and RNF170KO cells. B. GnRH (0.1μM)-induced Ca^{2+} mobilization in αT3 control and RNF170KO cells. C. IP_3R1 ubiquitination in αT3 control and RNF170KO cells. Cells were incubated with 0.1μM GnRH and anti-IP_3R1 IPs and input lysates were probed for the proteins indicated. D. IP_3R1 down-regulation in αT3 control and RNF170KO cells. Cells were incubated with 0.1μM GnRH and lysates were probed for the proteins indicated. The histogram shows combined quantitated immunoreactivity (mean±SEM, n=4). E. Reconstitution of IP_3R1 ubiquitination in RNF170KO cells. αT3 RNF170KO cells stably expressing $^{WT}RNF170$ or $^{R198C}RNF170$ were incubated without or with 0.1μM GnRH for 20min, and anti-IP_3R1 IPs were probed for the proteins indicated.

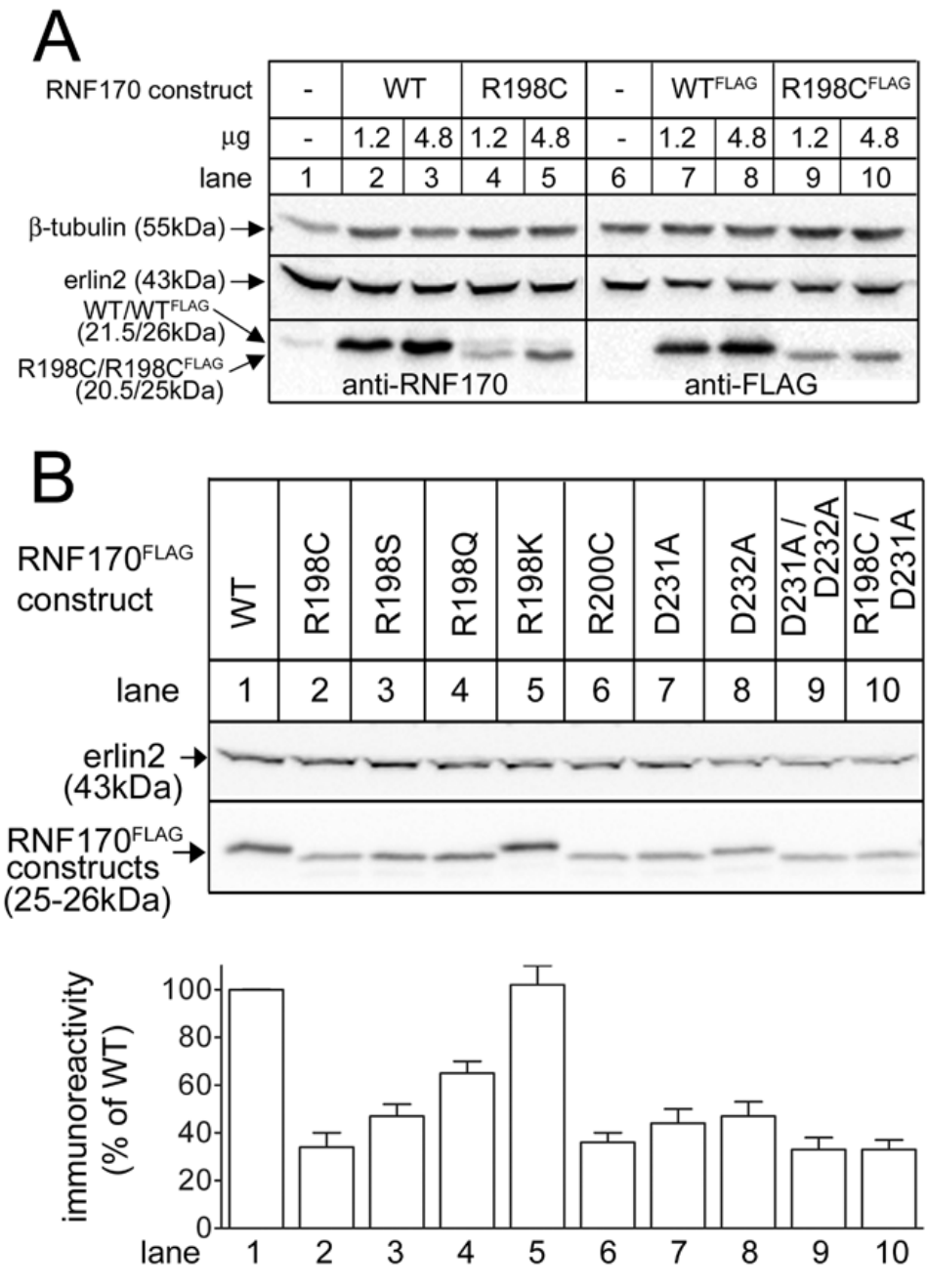
Downloaded from http://www.jbc.org/ at Shanghai Information Center for Life Sciences, Chinese Academy of Sciences on May 25, 2015

FIGURE 1



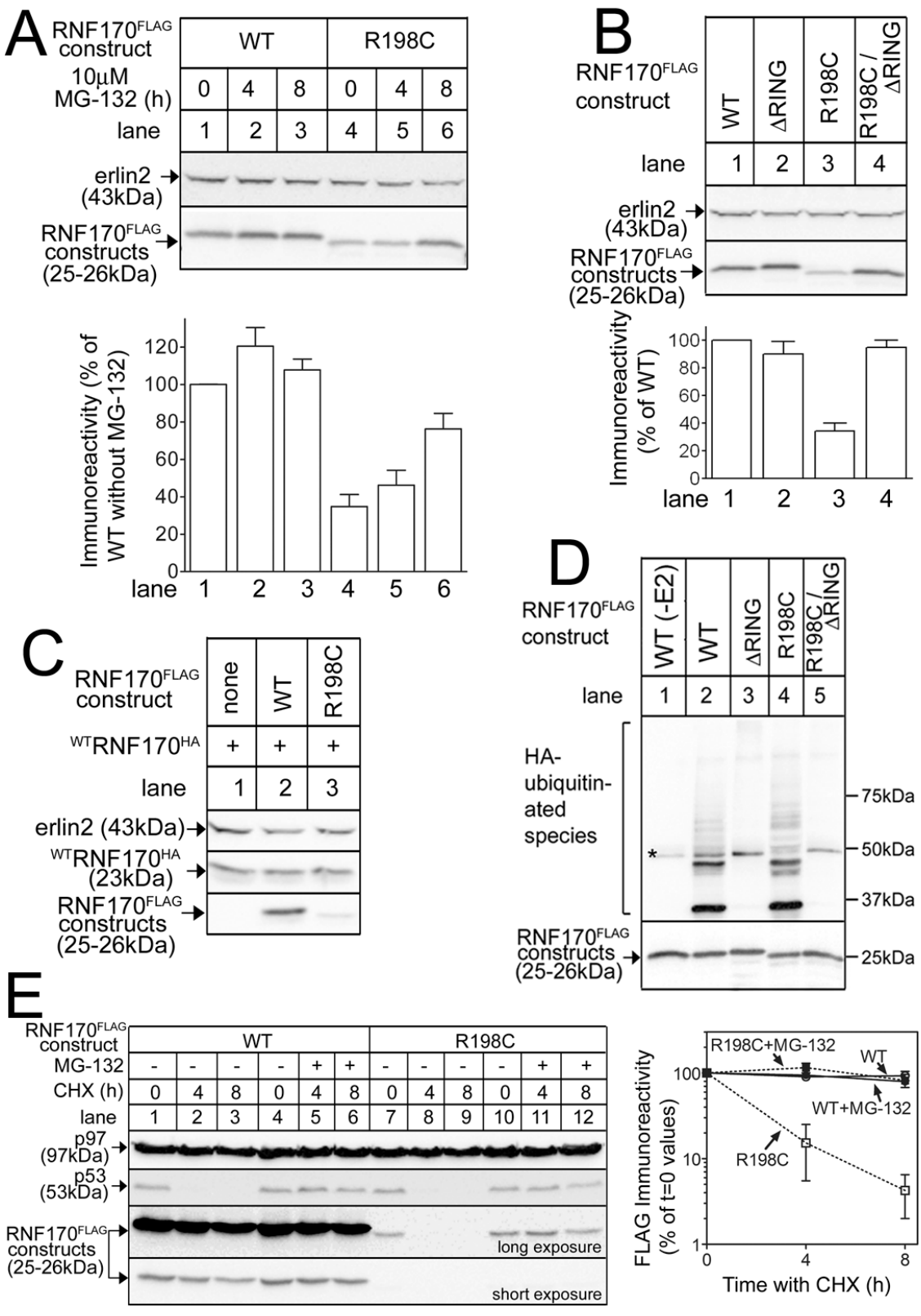
Downloaded from http://www.jbc.org/ at Shanghai Information Center for Life Sciences, Chinese Academy of Sciences on May 25, 2015

FIGURE 2



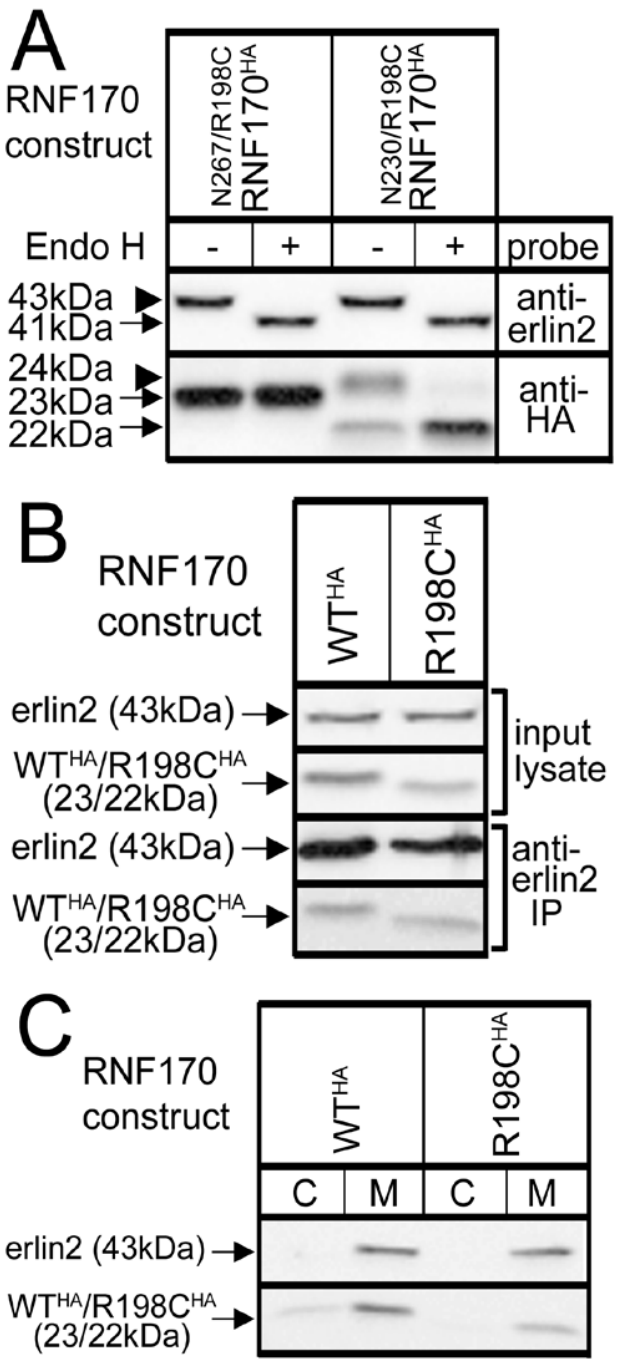
Downloaded from http://www.jbc.org/ at Shanghai Information Center for Life Sciences, Chinese Academy of Sciences on May 25, 2015

FIGURE 3



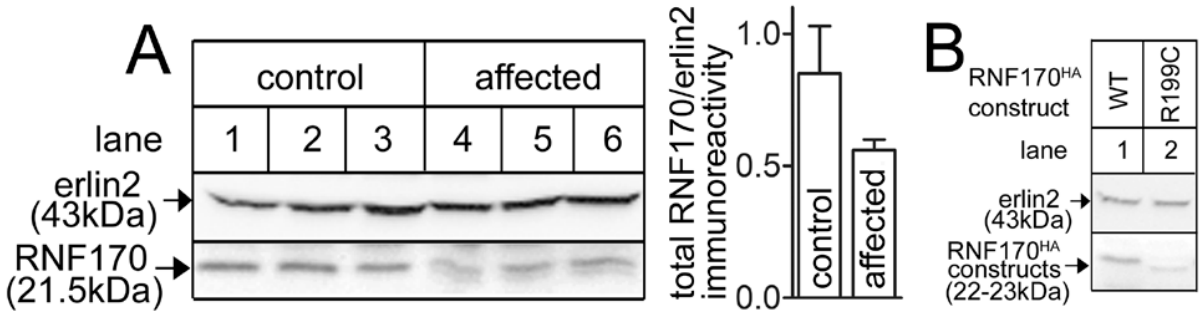
Downloaded from http://www.jbc.org/ at Shanghai Information Center for Life Sciences, Chinese Academy of Sciences on May 25, 2015

FIGURE 4



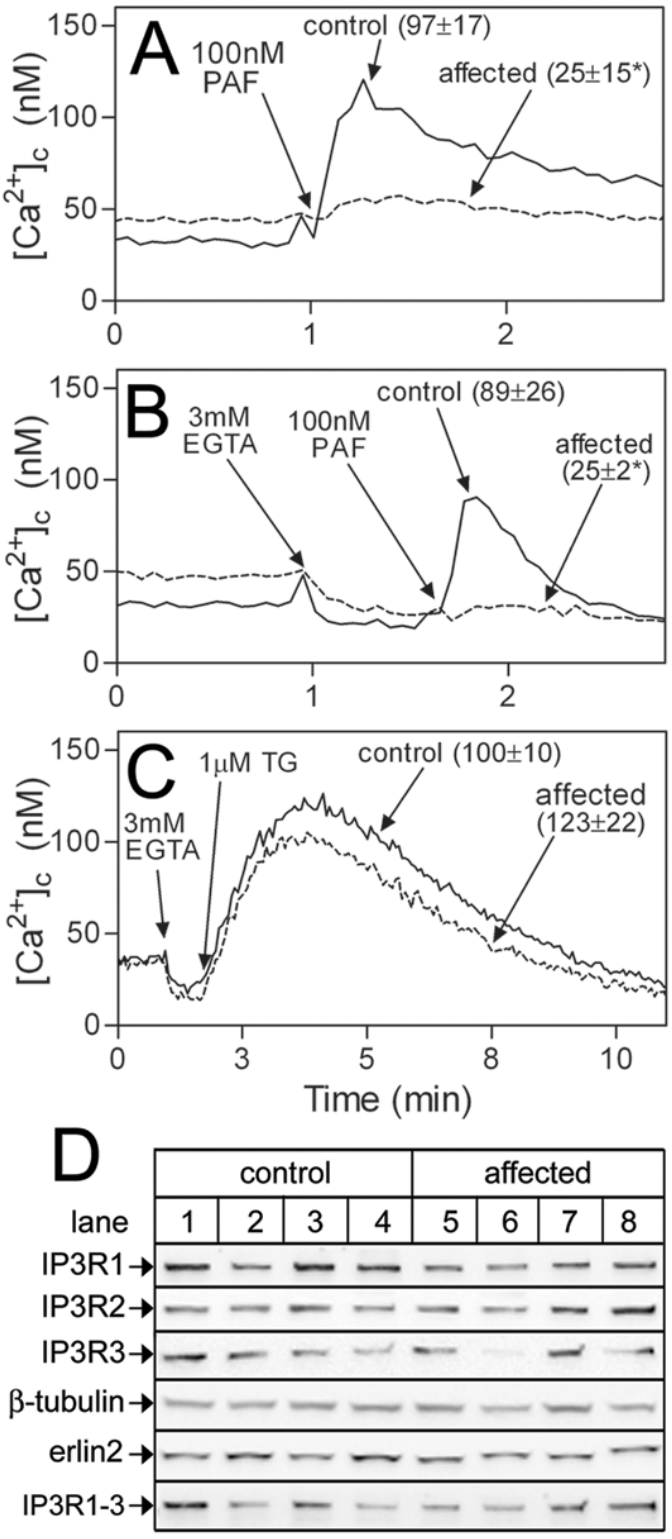
Downloaded from http://www.jbc.org/ at Shanghai Information Center for Life Sciences, Chinese Academy of Sciences on May 25, 2015

FIGURE 5



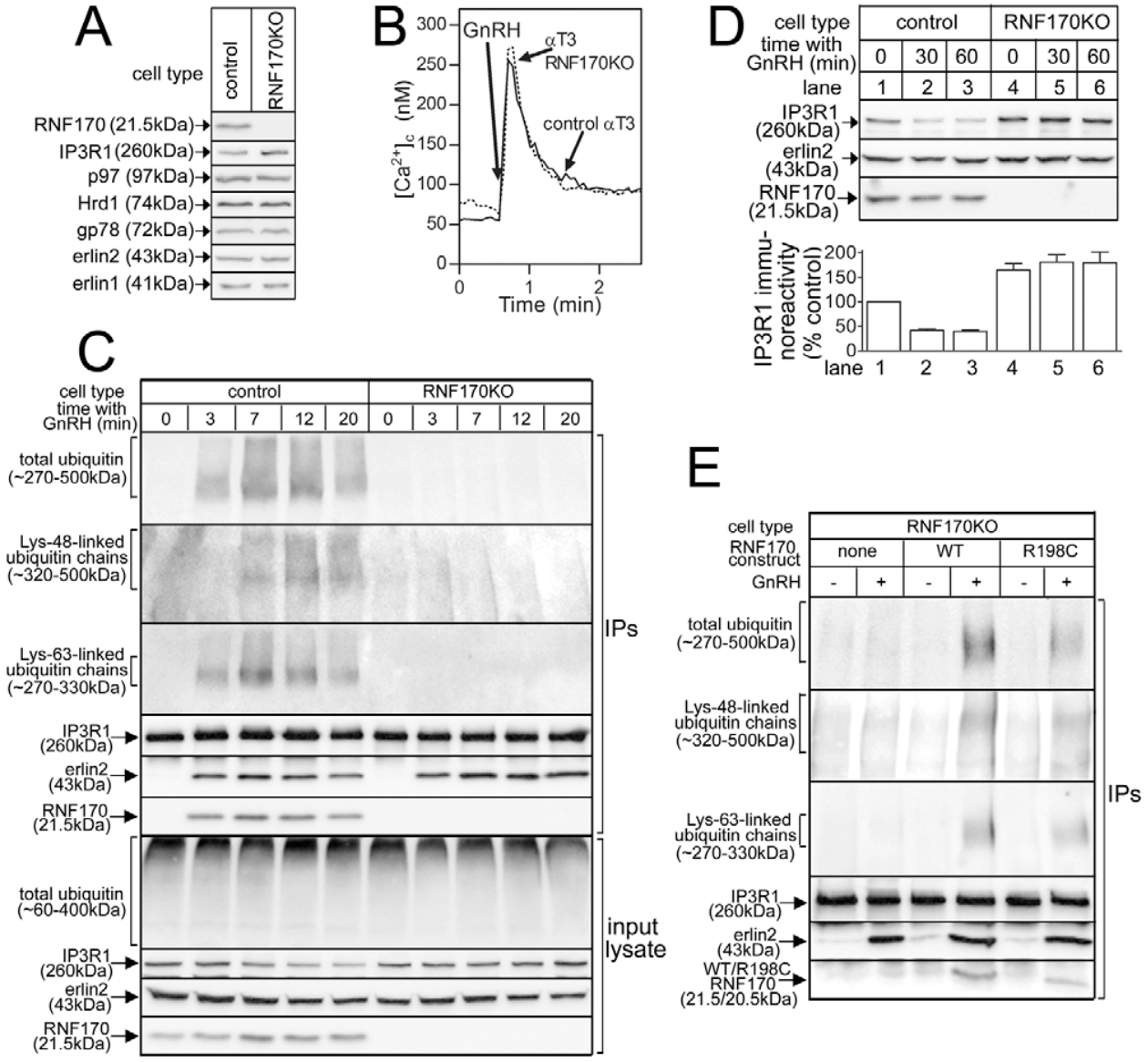
Downloaded from http://www.jbc.org/ at Shanghai Information Center for Life Sciences, Chinese Academy of Sciences on May 25, 2015

FIGURE 6



Downloaded from http://www.jbc.org/ at Shanghai Information Center for Life Sciences, Chinese Academy of Sciences on May 25, 2015

FIGURE 7

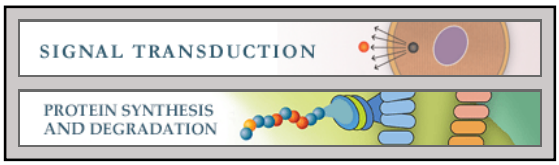


Downloaded from http://www.jbc.org/ at Shanghai Information Center for Life Sciences, Chinese Academy of Sciences on May 25, 2015



Signal Transduction:

A point mutation in the ubiquitin ligase RNF170 that causes autosomal dominant sensory ataxia destabilizes the protein and impairs inositol 1,4,5-trisphosphate receptor-mediated Ca2+ signaling



Forrest A. Wright, Justine P. Lu, Danielle A. Sliter, Nicolas Dupre, Guy A. Rouleau and Richard J. H. Wojcikiewicz

J. Biol. Chem. published online April 16, 2015

Access the most updated version of this article at doi: 10.1074/jbc.M115.655043

Find articles, minireviews, Reflections and Classics on similar topics on the JBC Affinity Sites.

Alerts:
- When this article is cited
- When a correction for this article is posted

Click here to choose from all of JBC's e-mail alerts

This article cites 0 references, 0 of which can be accessed free at
http://www.jbc.org/content/early/2015/04/16/jbc.M115.655043.full.html#ref-list-1

Downloaded from http://www.jbc.org/ at Shanghai Information Center for Life Sciences, Chinese Academy of Sciences on May 25, 2015